Transportation Research Part D 104 (2022) 103193

Contents lists available at ScienceDirect

Transportation Research Part D

journal homepage: www.elsevier.com/locate/trd

Emissions impacts of electrifying motorcycle taxis in Kampala, Uganda

Max Vanatta [a], Bhavesh Rathod [b], Jacob Calzavara [b,c], Thomas Courtright [b,d], Teanna Sims [e], Étienne Saint-Sernin [f], Herek Clack [g], Pamela Jagger [b,h], Michael Craig [b,*]

[a] Integrative Systems and Design, University of Michigan, 1075 Beal Avenue, Ann Arbor, MI 48109-2112, USA
[b] School for Environment and Sustainability, University of Michigan, 440 Church Street, Ann Arbor, MI, 48109, USA
[c] Stephen M. Ross School of Business, University of Michigan, 701 Tappan Ave, Ann Arbor, MI 48109, USA
[d] A. Alfred Taubman College of Architecture and Urban Planning, University of Michigan, 2000 Bonisteel Boulevard, Ann Arbor, MI 48109, USA
[e] Department of Electrical and Computer Engineering, University of Michigan, 1301 Beal Ave, Ann Arbor, MI 48109, USA
[f] Zembo Electric Motorcycles, Plot 163 Mutesa II Rd, Kampala, Uganda
[g] Department of Civil and Environmental Engineering, University of Michigan, 2350 Hayward Street, Ann Arbor, MI 48109, USA
[h] Gerald R. Ford School of Public Policy, University of Michigan, 735 S. State St., Ann Arbor, MI 48109, USA

ARTICLE INFO

Keywords:
Air pollution
Boda-bodas
Economic dispatch
Electric vehicles
Energy transitions
Electric motorcycles
Hydropower
Low and middle-income countries
Motorcycle taxis
Transportation emissions
Uganda

ABSTRACT

Large fleets of motorcycle taxis in Kampala, Uganda, and other cities in low and middle-income countries (LMICs) emit significant local and global air pollutants. To reduce emissions, companies have started selling electric motorcycles. We quantify the use-phase emissions impact of electrifying motorcycle taxis by processing real-world trip and charging data from Kampala, then estimating charging-caused emissions with an economic dispatch model of the Ugandan power system. We then compare these emissions to tank-to-wheels estimates of conventional motorcycles over the same trips. We find that electrifying gas-powered motorcycle taxis would reduce carbon dioxide (CO_2), carbon monoxide (CO), nitrogen oxide (NO_x), and hydrocarbon emissions by 36%, 90%, 58%, and 99%, respectively, but increase sulfur oxide (SO_x), particulate matter 10 μm or less (PM_{10}), and particulate matter 2.5 μm or less ($PM_{2.5}$) emissions by 870%, 109%, and 97%, respectively. PM and SO_x emission increases stem from generation at bagasse and heavy fuel oil (HFO) point sources far from load centers. Additionally, we find seasonality of the charging associated emissions due to dominance of hydropower in the Ugandan grid. Overall, we find clear and potential local air pollution benefits of electrifying motorcycle taxis in Kampala.

1. Introduction

Emissions of air pollutants threaten the wellbeing of individuals and the climate, locally and globally (Brunetti et al., 2021; IPCC, 2014; Maggiore et al., 2020; Richards et al., 2021). For individuals in urban regions, these multiscale threats are compounded by the localized effects of energy associated emissions. This is particularly true in cities across low and middle-income countries (LMICs) where rapid urbanization has caused an increase in poor air quality (The World Air Quality Project, 2020; World Health Organization,

* Corresponding author.
E-mail address: mtcraig@umich.edu (M. Craig).

https://doi.org/10.1016/j.trd.2022.103193

2018), contributing to morbidity and mortality (Fann et al., 2013, 2012). In Kampala, Uganda for example, air pollution levels frequently exceed levels deemed safe for humans by the World Health Organization (WHO) (Airqo, 2020; World Health Organization, 2018) reaching five to six times the WHO limits (Kampala Capital City Authority, 2018; Kirenga et al., 2015).

The United Nations (UN) Sustainable Development Goals (SDGs) provide a framework for efforts to combat both the global and local crises linked to airborne pollution. At the global scale, SDG 13 (Climate Action) highlights the urgency of our climate crisis and the actions which must be undertaken to reverse it such as implementing climate-aware policies (United Nations, 2020). At a more local scale, SDG 11 (Sustainable Cities and Communities) aims to reduce premature deaths linked to pollution (United Nations, 2020), which are estimated at 7 million annually across the globe (World Health Organization, 2021). The primary means of reducing these deaths and significantly improving health outcomes is through reduced emissions (Berman et al., 2012; Fann et al., 2012; Heo et al., 2016). SDG 9 (Industry, Innovation, and Infrastructure) provides a specific focus for accomplishing this by reducing the emissions intensity, primarily of carbon dioxide (CO_2), for the same unit of productivity within a given industry (United Nations, n.d.).

One of the major emitters of local air pollutants, such as particulate matter (PM), within LMICs is the transportation sector. For instance, Kinney et al. (2011) observed an 85% reduction in $PM_{2.5}$ concentrations as they moved from a major intersection to 100 m away in Nairobi, Kenya. This sector includes millions of gas-powered motorcycles within cities across Africa, Southeast Asia, and South America (Ampersand Solar, 2020; Ehebrecht et al., 2018; Posada et al., 2011). Across the ten largest motorcycle markets in Asia in 2010, there were over 200 million two-and three-wheelers accounting for 66% of the total number of vehicles (Law et al., 2015; Posada et al., 2011). This number is expected to grow around 4.2% annually with countries like China, India, Indonesia, Pakistan, and the Philippines growing 10.4–23.5% annually (Posada et al., 2011). In Uganda between 2007 and 2014, the total number of motorcycles grew from 15,979 to 405,124, a third of total vehicles (UNECE, 2018). The use of motorcycles as taxis has been growing in cities within LMICs. In Kampala, Uganda, estimates place the number of motorcycle taxis, known locally as boda-bodas, around 40,000, nearly a tenth of the total estimated motorcycles in the nation (Ehebrecht et al., 2018). The increased popularity of the motorcycle for personal and taxi use is due to many factors including lower upfront costs, lack of regulation, and mobility in highly congested urban contexts (Posada et al., 2011; UNECE, 2018). While motorcycles are often seen as a more fuel-efficient alternative (Posada et al., 2011), motorcycle emissions have not kept pace with that of cars. For instance, Momenimovahed et al. (2014) experimentally estimate PM emissions are three to three hundred times larger per kilometer from four and two stroke engine motorcycles respectively than a car. Other pollutant emissions can be worse from 2-wheelers than cars as well, particularly nitrogen oxides (NO_x), carbon monoxide (CO), and hydrocarbon (HC) emissions (Ehebrecht et al., 2018; Farquharson, 2019; Vasic and Weilenmann, 2006).

In response to these concerns, a push for the implementation of electric motorcycles is rapidly growing in sub-Saharan African cities (Alternet Systems, 2019; Ampersand Solar, 2020; ICLEI Local Governments for Sustainability, 2019), with Rwanda even considering banning gasoline motorcycles (Bright, 2020). With so many motorcycles operating and providing necessary services and employment, transitioning is not an easy challenge to overcome. Beyond the questions of charging infrastructure, access to electric motorcycles, and normalization of electric motorcycles, understanding the true air quality and health benefits of electric motorcycles is crucial for policymakers and companies deploying motorcycles.

Prior research has found emission benefits of electrifying cars and buses in mostly high-income countries. In the United States, Choma et al. (2020) found that switching from a gas-powered car to an electric vehicle (EV) improved emissions within urban contexts even when a fossil fuel asset charged the EV. Similarly, in Toronto, Canada, Gai et al. (2020) found electrifying all gas-powered cars would improve air quality even if EV charging occurred entirely with natural gas. In Belgium, Rangaraju et al. (2015) found that EVs would emit less than gas-powered vehicles in a full life-cycle analysis, and that emissions benefits vary more when accounting for real-world driving versus standard drive cycles. Weldon et al. (2016) similarly found that driver behavior was critical in evaluating the implications of converting from gas to electric cars. Transit buses offer similar levels of study such as Rupp et al. (2019), which uses observed behaviors of gas and electric buses in Germany to compare the well-to-wheel (WTW) emissions using flat emission factors. Heinisch et al. (2021) similarly studied electric buses, but utilized a dispatch model which allocates electricity generators based upon demand, cost, and system constraints to more accurately evaluate the impacts that EV and bus charging could have on a Gothenburg's heating, energy generation and storage infrastructure.

Despite public and private shifts towards electrified motorcycle taxis and existing air quality concerns, research on environmental impacts of electric motorcycle deployment is lagging. Few studies quantify emissions of electric versus gas-powered motorcycles, and none do so while accounting for changes in power system operations induced by electric motorcycle charging. This is especially important for sub-Saharan African nation-wide power systems, many of which utilize generators fueled by heavy fuel oil, diesel, or bagasse (i.e., sugarcane or sorghum residues) with high emission rates of global and local air pollutants (IEA, 2019). Farquharson (2019) estimates emissions and health impacts of switching from gas-powered to electric motorcycles in Kigali, Rwanda. To estimate emission impacts, Farquharson uses average emission factors (AEFs), which equal total annual grid emissions divided by total annual electricity generation. A key disadvantage of AEFs is that they assume a given increase in load results in the same amount of emissions regardless of when that increase in load occurs. In reality, an increase in load will likely be served by different generators (and result in different emissions) depending on when it occurs. To partly address this disadvantage, Farquharson conducts sensitivities for the fuel types likely to be the marginal emitters in Rwanda. Farquharson finds that emissions in Kigali from NOx, CO, particulate matter 10 μm or less (PM_{10}), particulate matter 2.5 μm or less ($PM_{2.5}$), hydrocarbons (HC), and CO_2 would all be reduced by switching to electric motorcycles. However, peat-burning electricity generators as the marginal emitter could cause CO_2 emissions to increase from electrifying motorcycles. Koossalapeerom et al. (2019) compared CO_2 emissions between gas-powered and electric motorcycles using one emission factor across the Thai power system. Cherry et al (2009) performed a similar analysis for the use of e-bikes in China and found the emissions associated with the use of e-bikes was lower than that of gas-powered vehicles, but over an e-bike lifecycle it had a greater amount of lead pollution due to the battery usage. Ji et al. (2012) carried this further and highlighted the increases in emissions

such as $PM_{2.5}$ for e-bikes in China due to their dependance on coal. However, Ji et al. found decreased mortality from e-bikes despite increased emissions due to a lower intake fraction caused by emissions occurring at power plants, further from populations.

Overall, there is a dearth of research on the emissions impact of electrifying motorcycles, including motorcycle taxis despite their prevalence in cities across the globe. Our literature review yielded only one such paper set in the African continent. Moreover, no existing research combines observed travel data with a dispatch model of the power system, which can capture generator fleet changes in response to charging demand. Such a dispatch model can be particularly valuable in hydropower-dominated systems such as Uganda's, which generates roughly 90% of its electricity annually from hydropower (see Section 2.3.1 & SI.1 for more details). In such hydropower-dominated systems, sub-annual hydropower generation budgets can lead to significant heterogeneity in generator responses to increased demand across time, which dispatch models can capture. These responses can lead to large differences in marginal emissions for increases in demand, which average emission factors cannot capture. Furthermore, data to quantify marginal emission factors are not available for the Ugandan system.

To begin to fill this gap and provide much-needed information to private and public actors, we quantify the emission consequences of electrifying gas-powered motorcycle taxis in Kampala, Uganda. To quantify charging-related emissions, we use an economic dispatch model of the power system, which captures individual generator responses across the system to accommodate charging demands. To quantify motorcycle taxis operations, we use observed data on trips and charging from 80 motorcycle taxis operating in Kampala during 2020. By coupling our economic dispatch model with real-world motorcycle taxi data, we quantify and compare emissions associated with gas-powered and electric motorcycle taxi charging. We quantify emissions of seven pollutants: CO_2, CO, SO_x, NO_x, HC, PM_{10}, and $PM_{2.5}$. We test the robustness of our results to using AEFs, on-site solar for charging, and several power system operational uncertainties.

2. Materials & methods

We use observed data on electric motorcycle taxi trips and charging in Kampala, Uganda, to generate an hourly grid demand schedule and an estimated gas-powered motorcycle taxi equivalent behavior. By inputting the demand schedule into our economic dispatch model of Uganda's power system, we evaluate how charging affects grid emissions. The grid side emissions are then compared to modeled gas equivalent emissions for the same motorcycle taxi behavior to quantify the emissions consequences of electrifying motorcycle taxis. In both cases, we quantify on use-phase emissions, leaving a full life cycle analysis (LCA) for later work. This method can be broken into two processes: (1) gas-powered motorcycle taxi modeling and (2) energy demand and power system modeling (Fig. 1).

2.1. Motorcycle taxi modeling

2.1.1. Data

We use two observational datasets related to motorcycle taxi trips- a log of all battery swaps and the raw GPS data associated with each motorcycle taxi. Both datasets are provided by the electric motorcycle taxi company Zembo. The log of battery swaps is a recorded series of entries which include the timestamp of the swap, the incoming state of charge (SOC In), outgoing state of charge (SOC Out), battery identifier (ID), and motorcycle taxi ID. The data is recorded to an app using a QR code reader to scan incoming battery, outgoing battery, and motorcycle taxi. There were nearly 55,000 swaps between November 2019 and January 2021 for over 130 motorcycle taxis. We acquire Zembo's GPS data for the same motorcycles through the private SinoTrack web portal (SinoTrack, 2021). The raw GPS data for each motorcycle taxi was collected by an onboard GPS unit which continuously recorded time, latitude, longitude, and device state even outside of operational hours. The device state indicates whether the data point is valid or is invalid due to lack of reception. Out of the 7,431,972 GPS points available, on average 98% are valid per motorcycle taxi. GPS data was collected from 80 motorcycle taxis starting in July 2020.

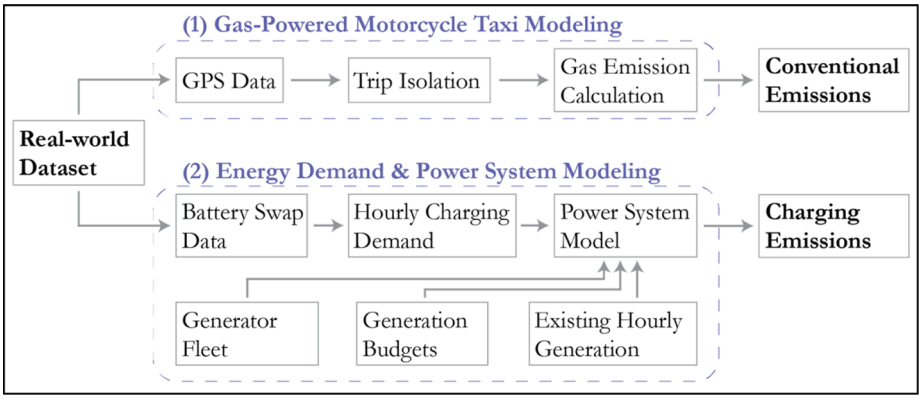

Fig. 1. Model Diagram of Our Emissions Modeling Pathways.

We clean the GPS datasets before converting them into trips in two steps. First, we ignore datapoints with a device state of 'invalid' for the remainder of the analysis because each GPS device defaults to a single GPS location when signal is lost regardless of where the previous accurate reading occurred. This step removes 2% of GPS entries on average from each motorcycle taxi's dataset and 1% of GPS entries across all motorcycle taxis, which we do not anticipate changing the overall understanding of driving behavior. Second, we assume that any point with a speed less than 2 km/hr is stationary but appearing as movement due to GPS drift. We choose this threshold because it accurately reproduces a driver's handwritten trip report. We find the speed between two time-adjacent valid points using the Haversine function.

To quantify and compare emissions from gasoline motorcycle taxis, which arise during trips, and electric motorcycle taxis, which arise during charging, we use internally-consistent GPS and battery swap data. To create internally-consistent data, we use *working weeks* in this study, which we define as a week with GPS and battery swap data. This yields GPS and charging data for 1,263 working weeks from 80 motorcycle taxis spanning July 13, 2020 to December 31, 2020. While there are social and cultural events that could result in non-representative operations in some of the working weeks in our sample set, e.g., around Christmas, our data suggests the distance traveled by drivers and variation within these weeks are similar to rest of the year (see boxplot in SI.3). Therefore, we do not treat any week uniquely. We characterize each existing motorcycle taxi by the average of its *working weeks*, providing an understanding of number of trips in a given timeframe, distance traveled per trip or timeframe, and charging demand per swap or timeframe.

2.1.2. Defining trips

We use GPS distances and speeds calculated above to divide our GPS data into discrete trips, where a trip is defined as a continuous period of time where a motorcycle taxi would be turned on and consuming energy. We assume this movement-based trip definition because we are primarily focused on the energy and fuel usage, and we do not have pick-up and drop-off data for most days. To create our trips, we progress through the GPS points until a speed value above 2 km/hr occurs, where we assume a trip has begun. We continue through the points until the speed value has been below 2 km/hr for over one minute, at which time the trip has ended. The process begins again, looking for the start of the next trip. We ground-truthed our cut-off period of 1 min with motorcycle taxi drivers, who stated that gas-powered motorcycle taxi drivers would shut their engines off beyond 1 min of not moving.

Once trips are separated, we calculate each trip's distance traveled, start time, end time, time duration, and time spent stationary (i.e., idle time). Additionally, for each trip we use start and end times to calculate the amount of time a motorcycle taxi is stationary before the trip and therefore whether the engine of a gas-powered motorcycle taxi would have a hot or cold start.

2.1.3. Motorcycle taxi charging data

Using real-world reported battery swap data, we build an hourly charging demand series for an entire year of motorcycle taxi usage. Motorcycle taxis used in this study use a 72 V 30 Ah Lithium Iron Phosphate (LFP) battery, which fully charges within two hours. Over this two-hour period, we assume a linear charge profile. The typical reported round trip efficiency (RTE) of LFP batteries is 92%, with non-ideal discharges sometimes incurring an RTE of 90% or lower (Bala et al., 2012; Eddahech et al., 2015; Pereirinha et al., 2012). We assume 90% to account for losses within the system. The LFP batteries used by the observed motorcycle taxis are 2.16 kWh. At a 90% RTE, these batteries require 2.4 kWh to charge from 0% to 100% state of charge (SOC). We leave incorporating the float charge or nonlinear charging of LFP batteries to future research, as changes in hourly demand due to these factors would be small and, due to the small battery size, dominated by uncertainty in how soon after the battery swap timestamp the battery is connected to the charger.

For each swap, we assume the battery starts charging at the swap timestamp at a constant rate of 1.2 kW until fully charged. We sum all the demand across motorcycle taxis and charging location into a total end-use demand for each hour of 2020 and incorporate an assumed 3.6% transmission loss (ERA, 2021a) and 16.4% distribution losses (Ministry of Energy and Mineral Development, 2020) resulting in 8,760 hourly demands on electricity generators.

2.2. Gas-powered emissions calculation

To understand emissions benefits of electric motorcycle taxi, we calculate what the emissions would have been if the defined trips were served by a gas-powered motorcycle taxi. The moving emissions are calculated using a per km emission factor, but the value of this depends on the stationary time prior to the trip beginning. If the vehicle had been stationary for more than 6 h, we assume a cold-start and therefore the initial emissions are higher than a hot-start condition (Yao et al., 2009). We also assume the emission rate

Table 1
Emission Factors for Gas-Powered Motorcycle Taxis.

Gas-Powered Motorcycle Taxi Emission Factors, 100 cc							
	CO_2	CO	NO_X	SO_X	PM_{10},	$PM_{2.5}$	HC
Hot Start [g/km]	55.5	2.17	0.08	0.0106***	0.018*	0.016*	0.38
Cold Start [g/km]	59.3	2.42	0.20	0.0106***	0.018*	0.016*	0.49
Idle [g/sec]	0.15**	–	–	–	-	–	–

All factors from Yao et al. (2009) unless otherwise noted.
* EPA MOVES Model (Office of Transportation and Air Quality, 2020).
** Nguyen et al., 2021.
*** Chester and Horvath, 2009.

linearly progresses from the cold-start emission rate to the hot-start emission rate over a period of 4 km (distance traveled in Yao et al. (2009)) due to lack of a more detailed relationship. All other trips are assumed to be hot-start emissions rates for the full duration. We calculate idle emissions based on a single time-based emission factor rather than hot or cold start values regardless of the location of the idle within a trip or the amount of stationary time prior to the trip (Table 1). Finally, we sum all moving emissions and idle emissions for a trip to find the total trip emissions. The values we present in Table 1 are not specific to motorcycles in Uganda but are instead primarily based upon experimentally observed vehicles abiding by Taiwan Environmental Protection Administration, Phase IV standards (Yao et al., 2009). We use these values for our analysis for two reasons: (1) they were the only readily available hot/cold start emissions parameters for the majority of pollutants, and (2) more specific emissions rates based upon model and age of typical motorcycles in Uganda were not available. Draft Ugandan motorcycle emissions standards for three of our pollutants (CO, NO_x, and HC) (UNBS, 2021), exceed the values from Yao et al. However, those standards are still in draft form and it is uncertain how well motorcycles adhere to those standards (Ayetor et al., 2021). Given these shortcomings, we use the values from Yao et al., possibly underestimating conventional motorcycle taxi emissions and emissions benefits of electrification.

2.3. Power system modeling

To quantify power system emissions associated with charging the electric motorcycle taxis, we model power system operations using an economic dispatch (ED) model of the Ugandan power system. We use an ED model rather than an average emission factor method because the emissions associated with charging are not evenly distributed across all generators operating throughout the year, but instead are caused by the marginal generator at the time of charging which cannot be captured by the AEF. Additionally, there is no readily available data for the marginal emission factor (MEF) in Uganda which would capture this time temporally specific emission rate. Therefore, using the ED model we are able to more accurately link additional emissions to the additional load. This is particularly important for the Ugandan power system because it generates most of its electricity from emission-free hydropower, but also includes high emission peaking plants (see Section 2.3.1) that may disproportionately serve increasing load. The difference between these two methods is demonstrated in Section 3.3.1. The ED model is a linear optimization that minimizes total system variable costs while enforcing generator- and system-level constraints. Our ED is formulated as follows:

$$minimize \sum_t c_t \tag{1}$$

$$s.t.: \quad c_t = \sum_i x_{i,t} \times (VOM_i + HR_i \times FC_i) \quad \forall i \in I, t \in T \tag{2}$$

$$D_t \leq \sum_i x_{i,t} \quad \forall i \in I, t \in T \tag{3}$$

$$0 \leq x_{i,t} \leq X_i^{MAX} \quad \forall i \in I, t \in T \tag{4}$$

$$x_{i_s,t} \leq XS_{i_s,t}^{MAX} \quad \forall i_s \in I_s, t \in T \tag{5}$$

$$\sum_{t_q} x_{i_h,t_q} \leq XH_{i_h,q}^{MAX} \quad \forall i_h \in I_h, t_q \in T_q, q \in Q \tag{6}$$

where i, t, i_s, i_h, t_q, and q index electricity generators, hours, solar generators, hydropower generators, hours per quarter, and quarters, respectively; c = hourly system operational costs [$]; x = electricity generation [MWh]; VOM = variable operation and maintenance cost [$/MWh]; HR = heat rate [MMBtu/MWh]; FC = fuel cost [$/MMBtu]; D = system-wide hourly demand [MWh]; X^{MAX} = maximum generation capacity [MWh]; XH^{MAX} = quarterly (3-month) hydropower electricity generation budget [MWh]; and XS^{MAX} = hourly maximum solar generation [MWh].

We run our ED model for each hour of the year but divide the year into quarters to accommodate seasonal hydrological budgets (see Section 2.3.1). We ignore ramping and reserve margins in this study due to data limitations. We implement our ED model in Python and solve it using the interior-point method in Scipy (Virtanen et al., 2020). Key inputs to the ED model are the generator fleet, generation limits, and demand, which we describe below. Validation of the ED model is located in Supplemental Materials SI.2.

2.3.1. Uganda power system description

The Ugandan fleet is composed of large hydroelectric power plants (LHPPs) (855 MW in total), small hydroelectric power plants (SHPPs) (148 MW in total), heavy fuel oil thermal power plants (HFO) (100 MW in total), bagasse cogeneration (combustion of the byproduct pulp residue of sugarcane) (44 MW in total), and grid connected solar (60 MW in total) (London Economics International, 2021). We do not consider import and export directly within the model, but export is already encapsulated in the hourly and yearly generation data described later in this section. Furthermore, Ugandan imports did not exceed 10.5 MWh in any of the 54 h of imports in 2017 (Bujagali Energy Limited and Government of Uganda, 2019), a small share of total generation. Due to data limitations, we estimate variable costs for generators based on their technology type. We estimate variable costs for solar, SHPP, LHPP, bagasse, and HFO as $2.4/MWh (World Bank, 2007), $3.5/MWh (World Bank, 2007), $4.41/MWh (World Bank, 2007), $52.53/MWh (IRENA, 2012; Isabirye et al., 2013; World Bank, 2007), and $451.01/MWh (Engineering ToolBox, n.d.; IEA, 2020; Qatar Petroleum, n.d.;

Table 2
Generation emission factors for all emitting fuel types on the Ugandan grid.

Emission Factors (kg/MWh)								
		CO_2	CO	NO_X	SO_X	PM_{10}	$PM_{2.5}$	HC
Bagasse Cogeneration	Primary Value	1,950 (EPA, 1993)	16.3 (Quintero et al., 2008)	1.52 (Quintero et al., 2008)	0.45[c] (Irfan et al., 2014)	2.29[a] (EEA, 2019)	1.96[a] (EEA, 2019)	0.27[a,d] (Eggleston et al., 2006)
	Low Value	1,520 (EPA, 1993)	8.13[b]	0.6 (EPA, 1993)	0.10[a] (EEA, 2019)	1.14[a] (EEA, 2019)	0.97[a] (EEA, 2019)	0.09[b] (Eggleston et al., 2006)
	High Value	2,380 (EPA, 2018)	31.0 (Irfan et al., 2014)	6.43 (Irfan et al., 2014)	0.68[b]	4.57[a] (EEA, 2019)	3.92[a] (EEA, 2019)	0.90[b] (Eggleston et al., 2006)
HFO Thermal Plant	Primary Value	696 (Eggleston et al., 2006)	0.22 (EEA, 2019)	2.09 (EEA, 2019)	7.30 (EEA, 2019)	0.37 (EEA, 2019)	0.28 (EEA, 2019)	0.03[d] (Eggleston et al., 2006)
	Low Value	635 (Bujagali Energy Limited and Government of Uganda, 2019)	0.13 (EEA, 2019)	0.92 (EPA, 2010)	6.61 (EPA, 2010)	0.28[e] (Lehtoranta et al., 2019)	0.02 (EEA, 2019)	0.01[d] (Eggleston et al., 2006)
	High Value	718 (Juhrich, 2016)	0.32 (Sandmo, 2013)	6.75 (Sandmo, 2013)	28.7 (Sandmo, 2013)	0.85[e] (Lehtoranta et al., 2019)	2.21 (EEA, 2019)	0.09[d] (Eggleston et al., 2006)

We use the primary value for all scenario results and the low/high values for the emission factor sensitivity analysis (Section 3.3.2).

[a] Non-bagasse specific, instead is labelled 'Agricultural Byproducts' and 'Biomass'.

[b] When multiple values were not found for the pollutant, the single value had a 50% buffer added on either side.

[c] SO2 value used for SOx emissions.

[d] Using CH4 reported values.

[e] Shipping emissions rather than stationary source.

Table 3
Sensitivity analyses descriptions and rationales.

Sensitivity Analysis	Parameters or Methods Varied	Rationale
AEF-Derived Results	ED model emissions results vs. 2019 system-wide AEF (102 kg CO_2/MWh) derived emissions for the 1,000 motorcycle taxi scenario.	We quantify the AEF-derived emissions and compare them to the ED model results to evaluate and demonstrate the utility of a power system model compared to method used in previous studies (Section 1)
Generation Emission Factors (EFs)	HFO & bagasse generation emission factors (values in Table 2)	Since we do not have observed all generator EFs, we use generic EFs by plant-type from the literature. These generic EFs vary significantly across references, so we quantify how different assumed EFs change charging emissions.
On-Site Solar Utilization	Installed capacity of on-site solar directly charging batteries: 0 to 5 kW_{Solar}/motorcycle taxi in 0.5 kW_{Solar}/motorcycle taxi increments.	On-site solar is increasingly common, so we evaluate how on-site installation for charging batteries changes charging emissions.
'Must-run' HFO	HFO minimum power: 0 MW (scenarios) and 2.5 MW (5% CF minimum)	Our model assumes purely economic dispatch, but HFO is considered 'must-run' by the ERA (Bujagali Energy Limited and Government of Uganda, 2019). We evaluate the impacts a minimum generation requirement has on charging emissions.
Hydrological Budgets	Generation Budgets for LHPP, SHPP, and Bagasse ranging from a typical *Wet* year to *2x Dry* year. *Wet year* budget: Based on 2018 Quarterly Generations (ERA, 2019). *Dry year* budget: Based on 2014 Quarterly Generations (ERA, 2019). For detailed budgets, see Supplemental Materials SI.4.4	Meteorological, hydrological, and policy factors drive the generation budgets underlying the ED model. We evaluate how inter-annual variability in these budgets changes charging emissions.

Rossol et al., 2018; World Bank, 2007), respectively. We also allow for non-served energy in the ED model at a cost of $1,000/MWh. For more generator fleet and cost details, see Supplemental Materials SI.1.

Potential electricity generation from hydropower plants, which provide the backbone of the Ugandan power system, vary with meteorological, hydrological, and policy conditions. Uganda has two rainy seasons, March to May and September to November, and two dry seasons (Kyatengerwa et al., 2020). To limit potential hydropower generation given observed natural and policy driven seasonality, we define quarterly generation budgets: Q1, Jan-Mar; Q2, Apr-Jun; Q3, Jul-Sep; Q4, Oct-Dec for each of the four LHPPs and aggregate SHPP. We sum available 2020 monthly generation data for the three of the four LHPPs (Isimba, Bujagali, and Eskom) to estimate quarterly generation per LHPP (UETCL, 2020a). There is not 2020 monthly data available for the fourth LHPP (Achwa II). To estimate the quarterly generation of Achwa II, we find the quarterly capacity factor for each of the other three LHPPs; average the three LHPPs' capacity factors each quarter; then multiply the quarterly average capacity factor by the nameplate capacity of Achwa II and the hours in a quarter. Unlike LHPPs, no 2020 data exists for SHPPs. Instead, the most recent year of generation data for SHPP is 2018. To estimate SHPP quarterly generation, we first quantify 2018 quarterly capacity factors across all operating SHPP generators, then multiply these capacity factors by the 2020 total nameplate capacity of SHPP and the number of hours in each quarter.

Potential generation from bagasse combustion and solar power are also constrained by biomass feedstock and solar resources, respectively, which we capture. For bagasse, we use the 2018 reported quarterly generation (ERA, 2019) for our budgets. For solar, we estimate hourly resource limits using the National Solar Radiation Database (NSRDB) (Sengupta et al., 2018) and PVWatts (NREL, n. d.). We obtain site-specific solar resources from NSRDB using the latitude and longitude of each solar plant. Using site-specific hourly solar resource and nameplate capacities, we calculate site-specific hourly generation using PVWatts. In the absence of plant-specific data, we use default PVWatt assumptions regarding plant parameters, including a 1.1 inverter loading ratio (ILR), 96% inverter efficiency, and 14% system losses. While HFO is considered 'must-run' by the ERA (2019) and seen to operate at a fairly consistent 7% capacity factor throughout the year (UETCL, 2020a), we assume a purely economic dispatch model and as such HFO behaves as a peaking generator, but we test the sensitivity of our results to enforcing a must-run HFO policy (see Section 3.4.2).

For the power system model, we balance supply and demand each hour, requiring hourly total system demand. Since hourly demand is not available, we estimate it as historical hourly generation accounting for transmission and distribution losses. Thus, we neglect existing unserved loads, which have been reported (UETCL, 2020b). Unserved load is a nonnegligible issue for the Ugandan power system and is linked with transmission and distribution limitations more often than generator capacity (Akena, 2020). Modeling transmission and distribution limitations is beyond the scope of this work and therefore left for later investigation. To estimate historic demand, we use the most recent publicly available hourly generation profile from 2017 (Bujagali Energy Limited and Government of Uganda, 2019), then scale 2017 hourly generation in each quarter to match 2020 quarterly generation (UETCL, 2020a). This scaling maintains consistency between quarterly generation budgets and demand.

Our ED model yields hourly generation by generator. To calculate annual emissions, we sum generation by generator, then multiply annual generation by each generator's fuel-type-specific emission factor (Table 2). Only one emission factor is specific to generators in Uganda is publicly available, CO_2 from HFO. This value is 7% below the lower end of the range estimate of HFO CO_2 emissions factors from the IPCC (Eggleston et al., 2006). As a result, we use the Uganda-specific value as the low value in our sensitivity analysis and use the higher IPCC emission factor as our primary EF. For the remaining EFs, we collect emission factors from a variety of sources in high income nations and LMICs and evaluate the sensitivity of our results to these parameters in Section 3.3.2.

2.4. Scenarios and sensitivities

To quantify emissions benefits of electric versus gas-power motorcycle taxis, we run our analysis for four scenarios of motorcycle penetrations: 80, 250, 1,000, and 10,000. The existing penetration, 80 motorcycle taxis, is based upon each motorcycle's observed data over their own partial year scaled up to a full year of operation. Given ongoing growth in the electric motorcycle taxi fleet, we also consider the emissions consequences of larger motorcycle fleets, specifically of populations of 250, 1,000, and 10,000 motorcycles. As we do not have data available for these larger motorcycle fleets, we generate synthetic trip and charging data for them through a bootstrapping procedure. Specifically, we create annual trip and charging profiles for each motorcycle in the larger fleets by randomly sampling with replacement 52 *working weeks* of the 1,263 available. We repeat this process with a new random seed value for each

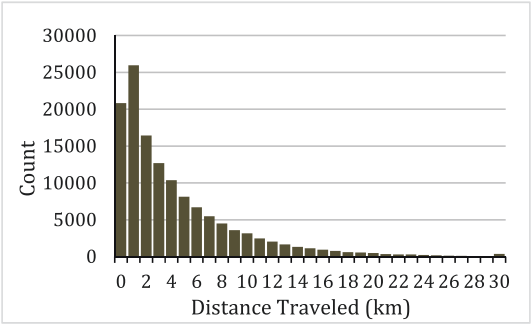

Fig. 2. Distance traveled per trip. All values greater than 30 are counted in the last column.

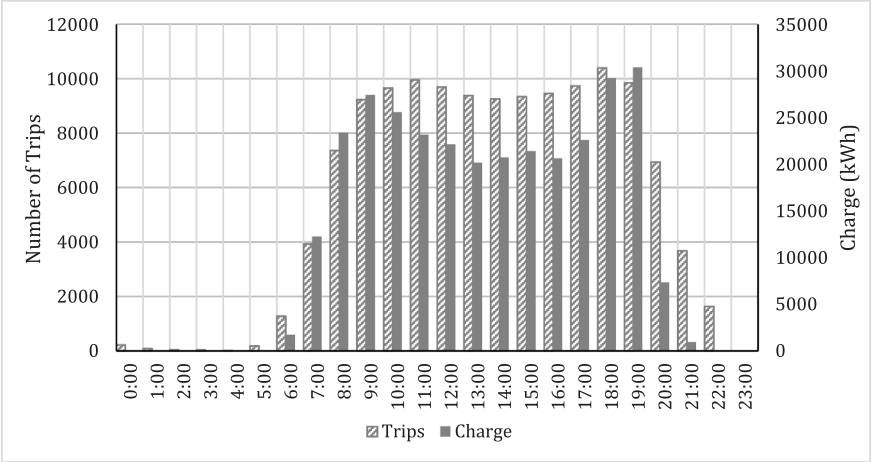

Fig. 3. Distribution of trips and charging throughout the day. These values are cumulative over the entire *working week* dataset. Trips, hatched, correspond to the left axis and Charge [kWh], grey, corresponds to the right axis.

synthetic motorcycle within the larger populations. For each of these scenarios, we compare CO_2, CO, NO_x, sulfur oxides (SO_x), PM_{10}, $PM_{2.5}$, and HC emissions associated with charging the electric motorcycle taxis to the emissions of a gas-powered motorcycle taxi on the same trips. We calculate the emissions associated with electric motorcycle taxis by adding the hourly generation demand for the charging in each scenario to the base Ugandan hourly demand, then running our ED model with this combined demand. We quantify charging emissions as the difference between annual emissions from base with the charging demand minus annual emissions from base demand alone. Given emission and power system uncertainties, we conduct several sensitivity analyses (Table 3).

3. Results

3.1. Motorcycle taxi trips and charging

Fig. 2 provides a histogram of distance traveled per motorcycle taxi trip using our observed data from 135,220 trips totaling 661,502 km. The average motorcycle taxi trip length was 4.92 km (4.89–4.94, 95% CI) and lasted 17.04 min (17.03–17.06, 95% CI). The distribution of trip distances is right-skewed, with a median value of 3.2 km (versus an average of 4.9). Motorcycle taxi trips are primarily short distances, with 1–2 km length trips accounting for the highest percent (20%) of trips. Based on personal observations, these short trips could capture trips easier via motorcycle than walking due to inadequate pedestrian infrastructure, movement from neighborhoods to larger arterial routes with minibuses, and non-customer trips such as moving from passenger drop-off to pick-up.

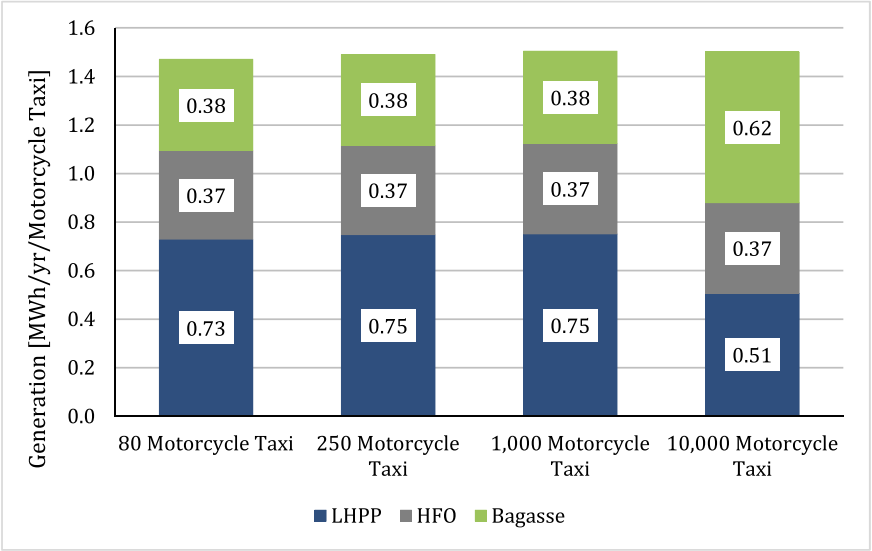

Fig. 4. Generation mix associated with the additional charging load. All data values on the bars are in MWh/year/motorcycle taxi.

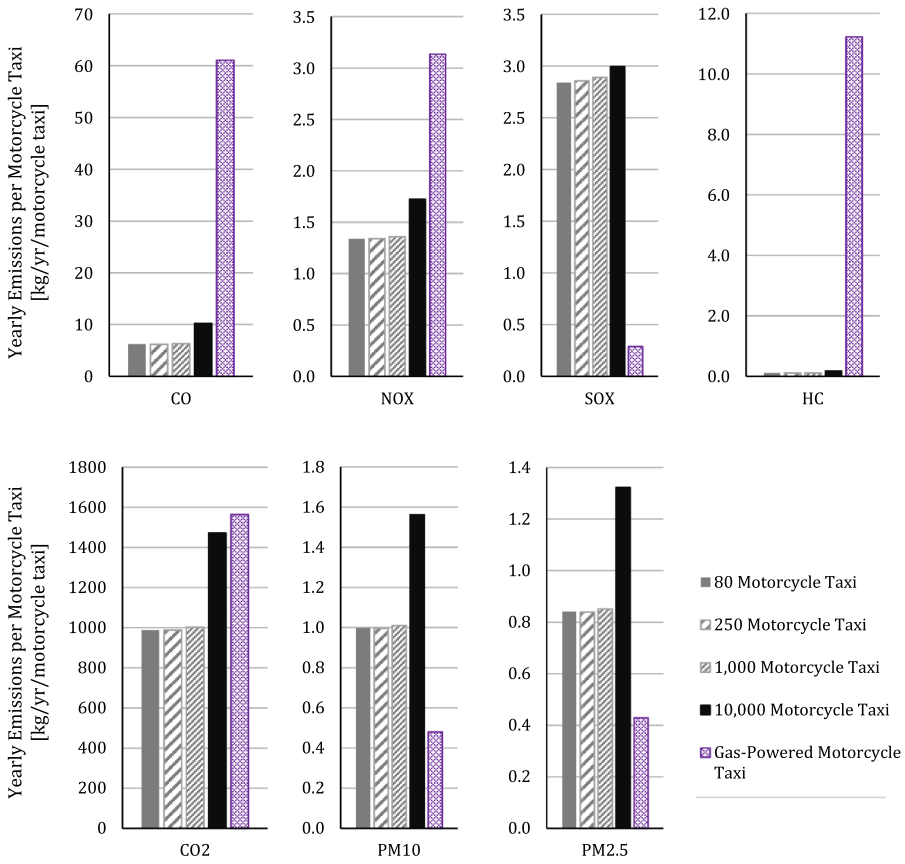

Fig. 5. Annual emissions (in kg) per motorcycle taxi across scenarios. Note differing y-axis scales between pollutants.

Only 2% of trips were longer than 20 km. Trips were distributed throughout the day growing sharply from 6 AM until 9 AM and remaining high until 7 PM, then declining to negligible levels through 11 PM. This aligns with the daily charging pattern, which peaks in morning and evening and negligible charging at night (Fig. 3). Based on observations in Kampala, the trips serve many purposes including deliveries and commuting, so occur at high levels throughout the entire day.

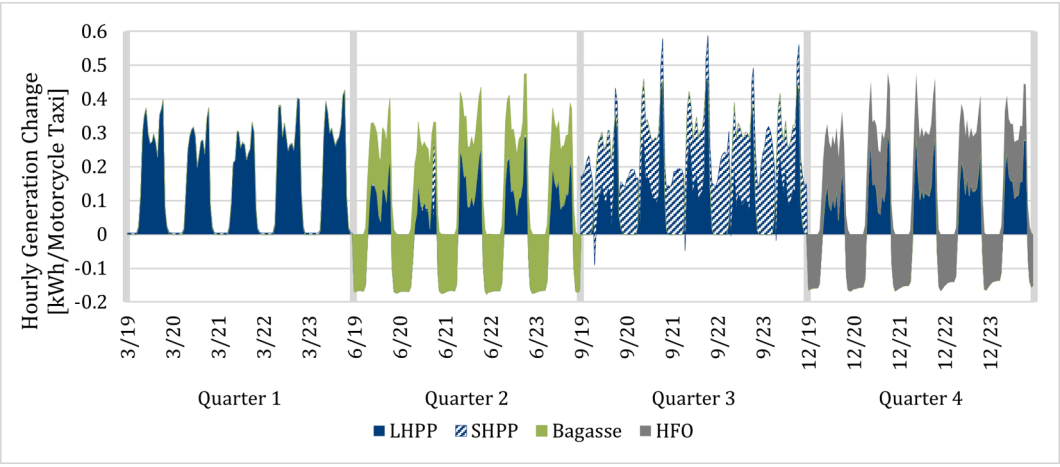

Fig. 6. Hourly difference in generation [kWh/motorcycle taxi] by source to charge a single motorcycle taxi in the 1,000 motorcycle taxis scenario. In Q2 and Q4, increased LHPP generation in some hours is offset by decreased generation in other (typically nighttime) hours due to quarterly hydrological budgets (not shown). In Q3, the same occurs for SHPP. Additionally, the SHPP in Q3 is displaced from other days in the quarter, as SHPP sees no change overall due to charging.

On a weekly basis (n = 1,263), motorcycle taxis average 105 trips (97–113, 95% CI). Over these trips, each observed motorcycle taxi travels 516 km/week (471–561, 95% CI) and charges 22.6 kWh/week (20.3–24.9, 95% CI). The average distance traveled between battery swaps was 35.8 km 11.8–58.9 km, 5th-95th percentile) and the average SOC difference was 64.6% or 1.5 kWh (23%-94%, 5th-95th percentile). To generate a synthetic annual series of motorcycle taxi trips throughout a full year, we randomly sample from our population of motorcycle taxi working weeks (see Section 2.4). Based on these synthetic annual series, each motorcycle taxi in our existing population of 80 would travel 26,757 km over 5,482 trips (Supplemental Materials SI.3). This requires 1,210 kWh/year/motorcycle taxi of charging. Given transmission/distribution (T/D) losses (Section 2.3.1), this charging demand leads to 1,504 kWh/year/motorcycle taxi of additional demand on the Ugandan power system. As we model increasing numbers of motorcycle taxis, the above per-motorcycle taxi metrics remain fairly constant with only slight variation caused by the random sampling process (Supplemental Materials SI.3).

3.2. Motorcycle taxi emissions

Given charging demand of 1.50 MWh/year/motorcycle taxi, we run our ED model with and without this charging demand to estimate the electricity source for charging. We find charging demand is met by LHPP, bagasse and HFO generators, with each generator type meeting charging demand in a particular quarter in all scenarios except 10,000 motorcycle taxis. LHPP generators serve motorcycle taxi demand in Q1 and Q3, bagasse generators serve it in Q2, and HFO generators serve it in Q4. This seasonal allocation is due to the quarterly budgets and is discussed in Section 3.2.1. With the charging demand fairly evenly distributed throughout the year, LHPP, bagasse, and HFO serve 0.75 MWh, 0.38 MWh, and 0.37 MWh respectively (Fig. 4). As the load is served by primarily a single generator type in each season, the ratio of energy provided by these fuel types remains fairly constant as we increase the number of motorcycle taxis to 1,000.

Due to electricity generation changes, each motorcycle taxi's annual charging emissions total 1,002 kg CO_2, 6.2 kg CO, 1.3 kg NO_x, 2.9 kg SO_x, 1.0 kg PM_{10}, 0.8 kg $PM_{2.5}$, and 0.1 kg HC. Annual charging emissions per motorcycle taxi vary little (by ±6.6 kg CO_2, ±0.1 kg all others) between the 80, 250 and 1,000 motorcycle taxi scenarios. Gas-powered motorcycle taxis annually emit 1,560 kg CO2, 61 kg CO, 3.1 kg NO_x, 0.3 kg SO_x, 0.5 kg PM_{10}, 0.4 kg $PM_{2.5}$, and 11.2 kg HC with little variation (by ±1 kg CO and ±5 kg CO_2). Fig. 5 displays these annual emissions results. Thus, we estimate switching from gasoline to electric motorcycle taxis would reduce emissions of CO_2 by 36%, CO by 90%, NO_x by 58%, and HC by 99%, but would increase emissions of SO_x by 870%, PM_{10} by 109%, and $PM_{2.5}$ by 97%. On an annual basis, for every motorcycle taxi converted to electric, emissions would be reduced by 558 kg CO_2, 55 kg CO, 1.8 kg NO_x, and 11.0 kg HC but would be increased by 2.6 kg SO_x, 0.5 kg PM_{10}, and 0.4 kg $PM_{2.5}$.

In the 10,000 motorcycle taxi scenario, bagasse provides a greater share of electricity for charging than in the other scenarios. Specifically, of the 1.50 MWh charging demand per motorcycle per year, LHPP, bagasse, and HFO would contribute 0.51 MWh, 0.62 MWh, and 0.37 MWh respectively. An increasing share of bagasse-fired generation alters the emissions benefits of switching to electric motorcycle taxis: switching from gasoline to electric motorcycle taxis would reduce emissions of CO_2 by 6%, CO by 83%, NO_x by 44%, and HC by 98% but would increase emissions of SO_x by 900%, PM_{10} by 225%, and $PM_{2.5}$ by 209%.

3.2.1. Seasonality of emissions

Generation seasonality strongly influences emissions associated with charging motorcycle taxis. In the 80, 250, and 1,000 motorcycle taxis scenarios, charging emissions only occur during low hydroelectric budget quarters (Q2, Q4) when bagasse and HFO generation served charging demand (Figs. 6 and 7). Furthermore, charging-induced grid emissions mostly occur in Q2 when bagasse contributes to meeting charging demand. In the 1,000 motorcycle scenario, for example, 74%, 99%, 86%, 86%, and 90% of annual CO_2, CO, PM_{10}, $PM_{2.5}$, and HC emissions occur during Q2 (Fig. 7). Conversely, 94% of SO_x emissions occur during Q4 due to HFO's high SO_x emissions rate relative to bagasse. Similar results occur for the 10,000 motorcycle taxis scenario, but bagasse generation also serves charging demand in Q1, increasing grid emissions in that quarter. Even at 10,000 motorcycle taxis, though, all charging demand in Q3 is met by LHPP and SHPP, resulting in no charging-induced emissions in that quarter.

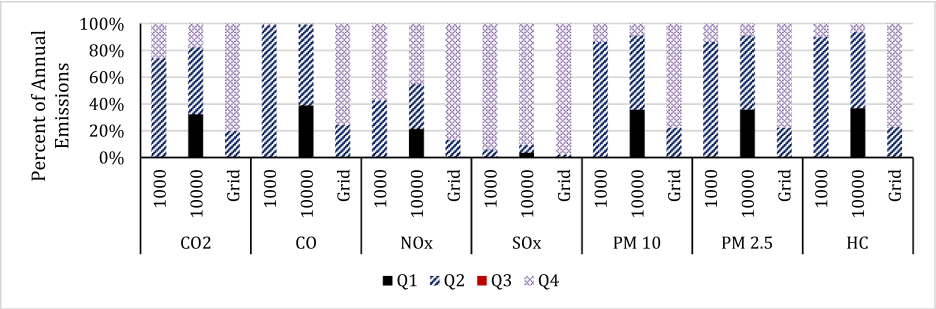

Fig. 7. Distribution of emissions between quarters. 80, 250, and 1,000 motorcycle taxis scenarios are all within a few percent and therefore solely the 1,000 motorcycle taxis scenario is presented as the representative scenario. Pre-charging, system-wide emissions are labeled as 'Grid' and shown for comparison to the additional loads of charging.

3.3. Sensitivity analysis

3.3.1. AEF derived results

We calculate the AEF as:

$$AEF = \frac{\sum_i EF_i \times x_i}{\sum_i x_i} \tag{7}$$

where i indexes generator technology; AEF = average emission factor [kg/MWh]; EF = emission factor [kg CO_2/MWh]; and x = electricity generation [MWh]. In 2019, the most recent year of data, bagasse, HFO, and hydropower (LHPP and SHPP) electricity generation totaled 197, 104, and 4,113 GWh, respectively (ERA, 2021b). Based on emission rates in Table 2, this generation mix yields which we used to calculate AEFs of 103 kg CO_2/MWh, 0.73 kg CO/MWh, 0.12 kg NO_x/MWh, 0.19 kg SO_x/MWh, 0.11 kg PM_{10}/MWh, 0.09 kg $PM_{2.5}$/MWh, and 0.01 kg HC/MWh. Using this simplified AEF method, we find that charging a single motorcycle taxi for a year would cause the emission of 155 kg CO_2, 1.10 kg CO, 0.18 kg NO_x, 0.29 kg SO_x, 0.17 kg PM_{10}, 0.14 kg $PM_{2.5}$, and 0.02 kg HC, versus our ED model result of 972 kg CO_2, 6.2 kg CO, 1.3 kg NO_x, 2.9 kg SO_x, 1.0 kg PM_{10}, 0.8 kg $PM_{2.5}$, and 0.3 kg HC. Thus, using an AEF to calculate charging-induced emissions would underestimate emissions by 82–90% depending on the pollutant.

3.3.2. Generation emission factors

Uncertainty in bagasse and HFO emission factors (EFs) (Table 2) most affect the relative value of electrifying motorcycle taxis for NO_x and PM emissions (Supplemental Materials SI.4.1). All other EF uncertainties do not qualitatively change our results. Using the high estimate for HFO NO_x EF would largely eliminate the NO_x benefits of electrifying motorcycle taxis that we previously observed (Section 3.2). The high estimate bagasse NO_x EF would increase NO_x emissions by 3%. With respect to $PM_{2.5}$ and PM_{10}, EF uncertainties do not qualitatively change our prior finding that electrifying motorcycle taxis would increase total $PM_{2.5}$ and PM_{10} emissions. However, the low range PM EFs for bagasse bring charging-induced emissions to within 19% and 10% of gas-powered motorcycle emissions for PM_{10} and $PM_{2.5}$ respectively.

3.3.3. On-site solar utilization

Using on-site solar for charging roughly equally displaces generation from LHPP, bagasse, and HFO generation sources, so reduces charging-induced emissions. Installation of 1 kW_{Solar}/motorcycle taxi reduces charging-induced emissions by roughly 60% (Supplemental Materials SI.4.2). Increasing solar deployment exhibits diminishing returns for the current charging schedule, such that deploying 5 kW_{Solar}/motorcycle taxi reduces charging-induced emissions by roughly 70%. These additional emission reductions occur during morning and evening charging times.

3.3.4. 'Must-run' HFO

HFO is considered 'must-run' by the ERA (ERA, 2019) and operates at a fairly consistent capacity factor throughout the year (UETCL, 2020a). Enforcing HFO as must-run in our ED model by setting its hourly minimum power output at 5% of its nameplate capacity (or at 2.5 MW) does not affect our results except in the 10,000 motorcycle taxis scenario. In that scenario, the must-run policy reduces charging-induced emissions to the level of the other three taxi scenarios (Supplemental Materials SI.4.3). The must-run policy increases HFO generation during Q1 by displacing LHPP generation, which frees up LHPP generation budget to charge the 10,000 motorcycle taxis. Q2 and Q4 emissions per motorcycle taxi remain the same due to the complete reliance on either bagasse or HFO for battery charging during these times.

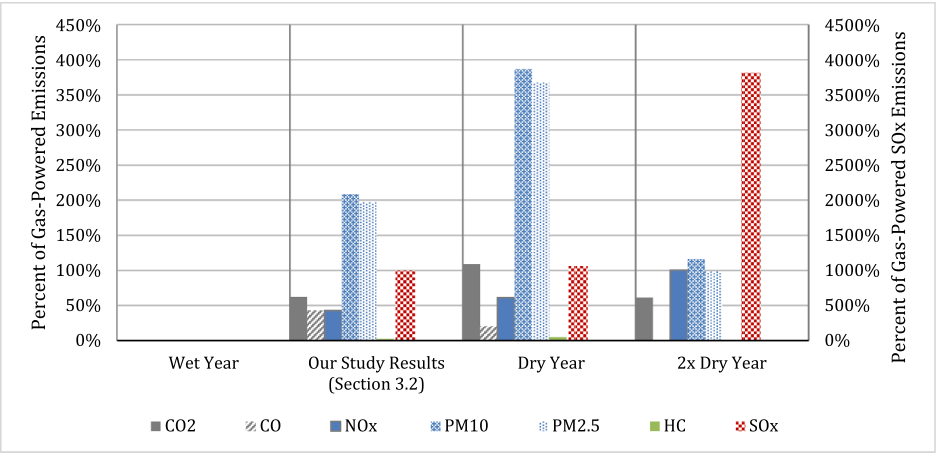

Fig. 8. Emissions under varying hydrological conditions for 1,000 motorcycle taxis scenario. SO_x emissions correspond to the right axis, all other pollutants to the left. The grey line shows the gas equivalent emissions for all pollutants except SO_x which has its reference line in red.

3.3.5. Hydrological budgets

Given the reliance of the Ugandan power system on hydropower, we test the sensitivity of our results to varying hydrological years. We find that motorcycle taxi charging can be served completely by hydropower in a *Wet* year compared to the 50% hydropower in our study results (Section 3.2). Once we hit a *Dry* year, only 25% of the charging load is served by hydropower with 50% served by Bagasse and 25% by HFO (Supplemental Materials SI.4.4). In drier conditions than the *Dry* budget, LHPP generation for charging continues to decline and is replaced first by bagasse generation and second by HFO generation. In conditions twice as dry as the *Dry* year, all charging load is served by HFO alone.

These changes in generation lead to changes in emissions. Across hydrological years, emissions of CO, NO_x, and HC would remain lower than or equal to gas-powered emissions (Fig. 8). Charging-induced emissions would be zero in the *Wet* year for all pollutants. CO_2 emissions could be greater than but within 10% of gas-powered emissions in a *2x Dry* year. In the *2x Dry* year, the SO_x emissions would reach their maximum at 3,800% of gas-powered equivalent. PM_{10} and $PM_{2.5}$ emissions would grow to above 350% during a *Dry* year due to the increased use of bagasse generation but would drop to nearly equal to the gas-powered equivalent in a *2x Dry* year as all generation is served by the HFO generators.

4. Discussion

In this study, we quantified how the transition from gas-powered to electric motorcycle taxis in Kampala, Uganda, would impact emissions by coupling real-world trip and charging data from 80 electric motorcycle taxis in 2020 with a power system dispatch model. For fleets of electric motorcycle taxis up to 1,000 taxis, we found that converting a gas-powered to electric motorcycle taxi would reduce annual emissions by roughly 588 kg CO_2, 55 kg CO, 2 kg NO_x, and 11 kg HC, but would increase annual emissions by 2.6 kg SO_x, 0.5 kg PM_{10}, and 0.4 kg $PM_{2.5}$. As a percent of gas-powered motorcycle taxi emissions, these changes equal reductions of roughly 38% of CO_2, 90% of CO, 58% of NO_x, and 97% of HC, and increases of roughly 870% SO_x, 109% PM_{10}, and 97% $PM_{2.5}$. For a fleet of 10,000 electric motorcycle taxis, emissions from electrified taxis are significantly greater for most pollutants, particularly PM_{10} and $PM_{2.5}$, due to greater bagasse-fired generation for charging.

Our results indicate that transitioning from gas-powered to electric motorcycle taxis would introduce trade-offs related to sustainability. Across all electric motorcycle taxi scenarios studied, we found electrifying motorcycle taxis would reduce CO_2 emissions. Thus, electrifying motorcycle taxis would make progress towards UN SDG 9.4 (United Nations, n.d.) and help mitigate climate change per UN SDG 13 (United Nations, n.d). Given that millions of gas-powered motorcycles are in use in cities across Africa, Southeast Asia, and South America (Ampersand Solar, 2020; Ehebrecht et al., 2018; Posada et al., 2011), our results suggest electrifying motorcycles in these locations could make a significant contribution to climate mitigation. Unlike for CO_2 emissions, we found electrifying motorcycle taxis would have mixed effects on local air pollutants. In particular, we found emissions of PM_{10} and $PM_{2.5}$ associated with charging electric motorcycles are close to double those of gas-powered motorcycles. These emission increases might undermine SDG 11.6.2, which aims to reduce PM levels in cities (United Nations, n.d), but this depends on the source of the emissions. In the case of electric motorcycles, bagasse power plants primarily responsible for PM emissions are located farther from population centers than gas-powered motorcycles, which are at street level. The closest bagasse plant to a population center is Kakira Sugar, which sits approximately 5 miles from Jinja and 40 miles from Kampala. Because power plants are farther from population centers than gas-powered motorcycles, the intake fraction of PM emissions would likely be lower from power plants than gas-powered motorcycles (Greco et al., 2007; Humbert et al., 2011). As a result, electrifying motorcycle taxis could improve health outcomes despite increasing total PM emissions. To that end, Ji et al. (2012) found electrifying bicycles increased total $PM_{2.5}$ emissions but improved health outcomes due to increased PM emissions occurring at coal-fired power plants far from population centers.

Similar to PM emissions, we found charging electric motorcycles increases emissions of SO_x compared to gas-powered motorcycles. This primarily comes down to the sulfur content of the two fossil fuels generating the energy for the motorcycle taxis. The international trend for gasoline is decreased sulfur content to prevent SO_x emissions. Many nations have regulations set at 30–300 ppm sulfur content in gasoline, correlating to a 0.03–0.3% sulfur composition of the fuel itself (Jaganathan, 2014; Transport Policy, n.d.). This is almost an order of magnitude smaller than the typical range of HFO sulfur composition of 0.1–4.5% (ExxonMobil, n.d.; Woodyard, 2009). However, HFO emissions (and bagasse emissions) can be controlled through point source emission controls, e.g. flue gas desulfurization, a more promising control route than improving emissions of hundreds of thousands of motorcycle taxis.

We performed several sensitivity analyses related to hydrological and power system uncertainties. Using AEFs instead of our ED model significantly underestimated CO_2 emissions associated with electric motorcycle taxis, as the AEFs miss seasonal hydropower generation constraints that require HFO and bagasse generation to meet some charging demand. This difference in ED model and AEF-derived results highlights the value of modeling the power system to evaluate charging emissions. Sensitivity analyses related to on-site solar deployment and a must-run HFO policy indicate both would reduce emissions from electric motorcycle taxis, making them more favorable relative to gas-powered motorcycles. Analyses related to variable hydrological years indicate significant sensitivity of electric motorcycle taxi emissions to hydrology with the exception of CO, NO_x, and HC emissions. Wet years generally reduce emissions, with the potential for near-zero charging emissions, while dry years generally increase emissions, with SO_x emissions exhibiting the greatest possible increase of up to 3,800% of gas-powered emissions in the driest conditions. Thus, the relative emission advantages of electrifying motorcycle taxis could vary significantly between years depending on hydrology, and could be significantly affected by future climate change.

Our results have several implications for policymakers in Uganda and other countries aggressively pursuing electric motorcycles like Rwanda (Bright, 2019). First, while our research quantifies emissions, air quality impacts are most relevant to human health. Understanding air quality impacts should therefore be a priority for future efforts sponsored by policymakers. However, our results

suggest electrifying motorcycle taxis would likely yield air quality benefits in Kampala, justifying support from policymakers. Second, we found that nuances of not only meteorological but also human-driven variations in hydropower usage throughout the year are of key importance when evaluating the emissions benefits of electrification. Given limited hydropower budgets, electrification of motorcycles will only yield deep emissions cuts for all pollutants if accompanied by supply-side actions. This interaction is crucial for policymakers to account for when considering electrification

5. Conclusions

Our research quantifies emissions for motorcycle taxis in Kampala, Uganda. Due to the specificity of our power system assumptions and underlying trip data, our results cannot be directly extrapolated to private motorcycles or other nations. However, our methods can be applied to private motorcycles or other nations by incorporating local parameters, and in turn improve our understanding of the factors that decision makers can or cannot manipulate to improve environmental and human health outcomes resulting from electric motorcycles.

Many opportunities for further research exist. In studying an electrified fleet of 10,000 motorcycle taxis, we assume no changes to the power system from its current composition. Given the time required for this number of electric motorcycle taxis to enter operation, this assumption will likely not hold. Additional emission-free hydropower or solar capacity could help meet the demand from these electrified motorcycle taxis and improve charging-associated emissions, which future research should explore. To that end, the generator fleet is rapidly growing, including 774 MW of hydropower and 50 MW of thermal construction in the next four years (London Economics International, 2021) though the long-term balance of fossil fuel versus hydroelectric could be impacted by recent oil and gas discoveries (U.S. Energy Information Administration, 2016). Transmission and distribution (T&D) limits can result in sub-optimal use of electricity generators in Uganda (Akena, 2020), which future research can embed within a dispatch model. New T&D projects in construction and planning will likely ameliorate these limits (UETCL, 2020c, 2020d); 51 million USD in T&D investments occurred during 2020 (Ministry of Energy and Mineral Development, 2020). Additionally, future research should move beyond emissions estimates to quantify air quality and public health benefits from electrifying motorcycle taxis. Finally, previous work has highlighted the concerns around resources and materials used in electric vehicles such as Cherry et al. (Cherry et al., 2009). Further research into the impacts of motorcycle electrification should incorporate a full life cycle analysis as our study solely considered use-phase emissions.

Overall, this research had three objectives: (1) quantify the emissions impact of transitioning from conventional gas powered to electric motorcycle taxis, (2) evaluate the benefits of calculating these impacts using an ED model, and (3) evaluate the robustness of these results across key uncertainties in EFs, grid constraints, and hydropower budgets. With respect to objective 1, our methods indicate electrifying motorcycle taxis can, at the system level, yield CO_2, CO, NO_x, and HC emission reductions concurrent with $PM_{2.5}$, PM_{10}, and SO_x emission increases. Through high spatiotemporal resolution, our methods further indicate $PM_{2.5}$ and PM_{10} emission increases will occur at a few point sources far from population centers, shifting PM and SO_x emissions away from populations and to point sources that decisionmakers could fit with emission controls. With respect to objective 2, we demonstrated that the use of an ED model for quantifying charging-induced emissions yields values six times higher than solely relying on average emission factors, which further provide a more complete assessment of charging associated emissions and allow for seasonality of emissions to be found. With respect to objective 3, we demonstrated our results are robust to uncertainties in EFs, generator policies, and yearly hydropower budgets with the opportunity to drive charging emissions even lower. Overall, these results indicate electrifying motorcycle taxis in Kampala can yield global sustainability benefits and, depending on air quality and health impacts, potentially local sustainability benefits.

Declaration of Competing Interest

The authors declare that they have no known competing financial interests or personal relationships that could have appeared to influence the work reported in this paper.

Acknowledgements

We would like to thank the University of Michigan Graham Sustainability Institute's funding through the Catalyst Grant. We would also like to thank the Zembo team and drivers for data and feedback.

Appendix A. Supplementary material

Supplementary data to this article can be found online at https://doi.org/10.1016/j.trd.2022.103193.

References

Airqo, 2020. Know your air. airqo.net.

Akena, A.K., 2020. Achievements and Challenges of Uganda's Power Sector [WWW Document]. RMI. URL https://rmi.org/achievements-and-challenges-of-ugandas-power-sector/ (accessed 6.20.21).

Alternet Systems, Inc., 2019. ALYI ReVolt electric motorcyle gains ground with Africa share of 218 billion shared rides. prnewswire.com.
Ampersand Solar, 2020. Ampersand Solar [WWW Document]. ampersand.solar. URL https://www.ampersand.solar/about (accessed 6.16.21).
Ayetor, G.K., Mbonigaba, I., Ampofo, J., Sunnu, A., 2021. Investigating the state of road vehicle emissions in Africa: A case study of Ghana and Rwanda. Transp. Res. Interdiscip. Perspect. 11, 100409.
Bala, S., Tengner, T., Rosenfeld, P., Delince, F., 2012. The effect of low frequency current ripple on the performance of a Lithium Iron Phosphate (LFP) battery energy storage system. In: 2012 IEEE Energy Conversion Congress and Exposition (ECCE). IEEE. https://doi.org/10.1109/ECCE.2012.6342318.
Berman, J.D., Fann, N., Hollingsworth, J.W., Pinkerton, K.E., Rom, W.N., Szema, A.M., Breysse, P.N., White, R.H., Curriero, F.C., 2012. Health Benefits from Large-Scale Ozone Reduction in the United States. Environ. Health Perspect. 120 (10), 1404–1410. https://doi.org/10.1289/ehp.1104851.
Bright, J., 2020. Rwanda to phase out gas motorcycle taxis for e-motos. TechCrunch.
Bright, J., 2019. Rwanda to phase out gas motorcycle taxis for e-motos | TechCrunch [WWW Document]. accessed 6.28.21 TechCrunch. https://techcrunch.com/2019/08/28/rwanda-to-phase-out-gas-motorcycle-taxis-for-e-motos/.
Brunetti, C., Dennis, B., Gates, D., Hancock, D., Ignell, D., Kiser, E.K., Kotta, G., Kovner, A., Rosen, R.J., Tabor, N.K., 2021. Climate Change and Financial Stability. FEDS Notes 2021. https://doi.org/10.17016/2380-7172.2893.
Bujagali Energy Limited and Government of Uganda, M. of E. and M.D., 2019. Bujagali Hydropower Project: Appendix 4: Baseline information and emission reductions calculations, Version 1.4.
Cherry, C.R., Weinert, J.X., Xinmiao, Y., 2009. Comparative environmental impacts of electric bikes in China. Transp. Res. Part D: Transp. Environ. 14 (5), 281–290. https://doi.org/10.1016/j.trd.2008.11.003.
Chester, M., Horvath, A., 2009. Life-cycle Energy and Emissions Inventories for Motorcycles, Diesel Automobiles, School Buses, Electric Buses, Chicago Rail, and New York City Rail. UC Berkeley Center for Future Urban Transport: A Volvo Center of Excellence UC Berkeley.
Choma, E.F., Evans, J.S., Hammitt, J.K., Gómez-Ibáñez, José.A., Spengler, J.D., 2020. Assessing the health impacts of electric vehicles through air pollution in the United States. Environ. Int. 144, 106015. https://doi.org/10.1016/j.envint.2020.106015.
Eddahech, A., Briat, O., Vinassa, J.M., 2015. Performance comparison of four lithium–ion battery technologies under calendar aging. Energy 84, 542–550. https://doi.org/10.1016/J.ENERGY.2015.03.019.
EEA, 2019. EMEP/EEA air pollutant emission inventory guidebook 2019: 1.A.1 Energy industries.
Eggleston, H., Buendia, L., Miwa, K., Ngara, T., Tanabe, K., 2006. 2006 IPCC guidelines for national greenhouse gas inventories. Japan.
Ehebrecht, D., Heinrichs, D., Lenz, B., 2018. Motorcycle-taxis in sub-Saharan Africa: Current knowledge, implications for the debate on "informal" transport and research needs. J. Transp. Geogr. 69, 242–256. https://doi.org/10.1016/j.jtrangeo.2018.05.006.
Engineering ToolBox, n.d. Fuels - Higher and Lower Calorific Values [WWW Document]. URL https://www.engineeringtoolbox.com/fuels-higher-calorific-values-d_169.html (accessed 6.24.21).
EPA, 2018. Emission Factors for Greenhouse Gas Inventories.
EPA, 2010. AP-42 VOL. I, Section 1.3 Fuel Oil Combustion, corrected May 2010.
EPA, 1993. EMISSION FACTOR DOCUMENTATION FOR AP-42 SECTION 1.8 BAGASSE COMBUSTION IN SUGAR MILLS.
ERA, 2021a. Energy Purchases, Sales and Losses [WWW Document]. URL https://www.era.go.ug/index.php/stats/transmission-stats/energy-purchases-sales-and-losses (accessed 6.22.21).
ERA, 2021b. Energy Generated [WWW Document]. URL https://www.era.go.ug/index.php/stats/generation-statistics/energy-generated (accessed 6.20.21).
ERA, 2019. Energy Generated in Mwh - 2018.
ExxonMobil, n.d. How IMO's sulphur cap decision will affect bunker supply chain: ExxonMobil Marine [WWW Document]. ExxonMobil: Marine. URL https://www.exxonmobil.com/en/marine/technicalresource/news-resources/imo-sulphur-cap-and-mgo-hfo (accessed 6.20.21).
Fann, N., Fulcher, C.M., Baker, K., 2013. The Recent and Future Health Burden of Air Pollution Apportioned Across U.S. Sectors. Environ. Sci. Technol. 47 (8), 3580–3589. https://doi.org/10.1021/es304831q.
Fann, N., Lamson, A.D., Anenberg, S.C., Wesson, K., Risley, D., Hubbell, B.J., 2012. Estimating the National Public Health Burden Associated with Exposure to Ambient PM2.5 and Ozone. Risk Analysis 32. https://doi.org/10.1111/j.1539-6924.2011.01630.x.
Farquharson, D.T., 2019. Sustainable energy transitions in sub-Saharan Africa: Impacts on air quality, economics, and fuel consumption. https://doi.org/10.1184/R1/9250325.v1.
Gai, Y., Minet, L., Posen, I.D., Smargiassi, A., Tétreault, L.-F., Hatzopoulou, M., 2020. Health and climate benefits of Electric Vehicle Deployment in the Greater Toronto and Hamilton Area. Environ. Pollut. 265, 114983. https://doi.org/10.1016/j.envpol.2020.114983.
GPS Tracking System [WWW Document], 2021. SinoTrack Inc. URL https://www.sinotrack.com/ (accessed 11.16.21).
Greco, S.L., Wilson, A.M., Spengler, J.D., Levy, J.I., 2007. Spatial patterns of mobile source particulate matter emissions-to-exposure relationships across the United States. Atmos. Environ. 41 (5), 1011–1025.
Heinisch, Verena, Göransson, Lisa, Erlandsson, Rasmus, Hodel, Henrik, Johnsson, Filip, Odenberger, Mikael, 2021. Smart electric vehicle charging strategies for sectoral coupling in a city energy system. Applied Energy 288, 116640. https://doi.org/10.1016/j.apenergy.2021.116640.
Heo, J., Adams, P.J., Gao, H.O., 2016. Reduced-form modeling of public health impacts of inorganic PM2.5 and precursor emissions. Atmos. Environ. 137, 80–89. https://doi.org/10.1016/j.atmosenv.2016.04.026.
Humbert, S., Marshall, J.D., Shaked, S., Spadaro, J.V., Nishioka, Y., Preiss, P., McKone, T.E., Horvath, A., Jolliet, O., 2011. Intake Fraction for Particulate Matter: Recommendations for Life Cycle Impact Assessment. Environ. Sci. Technol. 45 (11), 4808–4816. https://doi.org/10.1021/es103563z.
ICLEI Local Governments for Sustainability, 2019. Exploring informal sustainable mobility for East African cities. talkofthecities.iclei.org.
IEA, 2020. Key World Energy Statistics 2020. Paris.
IEA, 2019. International Energy Agency. Africa Energy Outlook 2019. World Energy Outlook Special Report. EA Publications.
IPCC, 2014. Climate Change 2014: Synthesis Report. Contribution of Working Groups I, II and III to the Fifth Assessment Report of the Intergovernmental Panel on Climate Change. IPCC, Geneva, Switzerland.
IRENA, 2012. RENEWABLE ENERGY TECHNOLOGIES: COST ANALYSIS SERIES, Green Energy and Technology.
Irfan, M., Riaz, M., Arif, M.S., Shahzad, S.M., Saleem, F., -Rahman, N.-ur., van den Berg, L., Abbas, F., 2014. Estimation and characterization of gaseous pollutant emissions from agricultural crop residue combustion in industrial and household sectors of Pakistan. Atmos. Environ. 84, 189–197. https://doi.org/10.1016/j.atmosenv.2013.11.046.
Isabirye, M., Raju, D.V.N., Kitutu, M., Yemeline, V., Deckers, J., Poese, J., 2013. Sugarcane Biomass Production and Renewable Energy. In: Matovic, M.D. (Ed.), Biomass Now – Cultivation and Utilization. InTech. https://doi.org/10.5772/56075.
Jaganathan, J., 2014. East Africa move to cleaner fuels to soak up new low-sulphur supplies. Reuters.
Ji, S., Cherry, C.R., J. Bechle, M., Wu, Y., Marshall, J.D., 2012. Electric vehicles in China: Emissions and health impacts. Environ. Sci. Technol. 46 (4), 2018–2024. https://doi.org/10.1021/es202347q.
Juhrich, K. (2016). *CO2 Emission Factors for Fossil Fuels, Emissions Situation (Section I 2.6)*. https://www.ipcc-nggip.iges.or.jp/EFDB/ef_detail.php.
Kampala Capital City Authority, 2018. Kampala's Air Quality Is Six Times Worse Than Global Standards -KCCA | For a better City [WWW Document]. URL https://www.kcca.go.ug/news/316/#.YPg-z-hKhPY (accessed 7.20.21).
Kinney, P.L., Gichuru, M.G., Volavka-Close, N., Ngo, N., Ndiba, P.K., Law, A., Gachanja, A., Gaita, S.M., Chillrud, S.N., Sclar, E., 2011. Traffic impacts on PM2.5 air quality in Nairobi, Kenya. Environ. Sci. Policy 14 (4), 369–378. https://doi.org/10.1016/j.envsci.2011.02.005.
Kirenga, B., Meng, Q., van Gemert, F., Aanyu-Tukamuhebwa, H., Chavannes, N., Katamba, A., Obai, G., Molen, T., Schwander, S., Mohsenin, V., 2015. The State of Ambient Air Quality in Two Ugandan Cities: A Pilot Cross-Sectional Spatial Assessment. Int. J. Environ. Res. Public Health 12 (7), 8075–8091. https://doi.org/10.3390/ijerph120708075.

Koossalapeerom, T., Satiennam, T., Satiennam, W., Leelapatra, W., Seedam, A., Rakpukdee, T., 2019. Comparative study of real-world driving cycles, energy consumption, and CO2 emissions of electric and gasoline motorcycles driving in a congested urban corridor. Sustainable Cities Soc. 45, 619–627. https://doi.org/10.1016/j.scs.2018.12.031.

Kyatengerwa, C., Kim, D., Choi, M., 2020. A national-scale drought assessment in Uganda based on evapotranspiration deficits from the Bouchet hypothesis. J. Hydrol. 580, 124348. https://doi.org/10.1016/j.jhydrol.2019.124348.

Law, T.H., Hamid, H., Goh, C.N., 2015. The motorcycle to passenger car ownership ratio and economic growth: A cross-country analysis. J. Transp. Geogr. 46, 122–128. https://doi.org/10.1016/J.JTRANGEO.2015.06.007.

Lehtoranta, K., Aakko-Saksa, P., Murtonen, T., Vesala, H., Ntziachristos, L., Rönkkö, T., Karjalainen, P., Kuittinen, N., Timonen, H., 2019. Particulate Mass and Nonvolatile Particle Number Emissions from Marine Engines Using Low-Sulfur Fuels, Natural Gas, or Scrubbers. Environ. Sci. Technol. 53 (6), 3315–3322. https://doi.org/10.1021/acs.est.8b05555.

London Economics International, 2021. Energy Mix Diversification Strategy For The Uganda Electricity Generation Company LTD ("UEGCL").

Maggiore, A., Afonso, A., Barrucci, F., Sanctis, G.D., 2020. Climate change as a driver of emerging risks for food and feed safety, plant, animal health and nutritional quality. EFSA Supporting Publications 17 (6).

Ministry of Energy and Mineral Development, 2020. Utilising Energy and Mineral Resources for Economic Recovery: Post Pandemic.

Momenimovahed, A., Olfert, J.S., Checkel, M.D., Pathak, S., Sood, V., Singh, Y., Singal, S.K., 2014. Real-time driving cycle measurements of ultrafine particle emissions from two wheelers and comparison with passenger cars. Int. J. Automot. Technol. 15 (7), 1053–1061.

Nguyen, Y.-L., Le, A.-T., Duc, K.N., Duy, V.N., Nguyen, C.D., 2021. A study on emission and fuel consumption of motorcycles in idle mode and the impacts on air quality in Hanoi, Vietnam. Int. J. Urban Sci. 25 (4), 522–541. https://doi.org/10.1080/12265934.2020.1871059.

NREL, n.d. PVWatts.

Office of Transportation and Air Quality, 2020. Motor Vehicle Emission Simulator: MOVES3.0.0.

Pereirinha, P.G., Trovão, J.P., Santiago, A., 2012. Set up and test of a LiFePO4 battery bank for electric vehicle. Przeglad Elektrotechniczny 88.

Posada, F., Kamakate, F., Bandivadekar, A., 2011. Sustainable Management of Two-and Three-Wheelers in Asia, ICCT.

Qatar Petroleum, n.d. ConversionFactor [WWW Document]. URL https://qp.com.qa/ar/Pages/ConversionFactor.aspx (accessed 6.24.21).

Quintero, J.A., Montoya, M.I., Sánchez, O.J., Giraldo, O.H., Cardona, C.A., 2008. Fuel ethanol production from sugarcane and corn: Comparative analysis for a Colombian case. Energy 33 (3), 385–399. https://doi.org/10.1016/j.energy.2007.10.001.

Rangaraju, S., de Vroey, L., Messagie, M., Mertens, J., van Mierlo, J., 2015. Impacts of electricity mix, charging profile, and driving behavior on the emissions performance of battery electric vehicles: A Belgian case study. Appl. Energy 148, 496–505. https://doi.org/10.1016/j.apenergy.2015.01.121.

Richards, C.E., Lupton, R.C., Allwood, J.M., 2021. Re-framing the threat of global warming: an empirical causal loop diagram of climate change, food insecurity and societal collapse. Clim. Change 164 (3-4). https://doi.org/10.1007/s10584-021-02957-w.

Rossol, M., Brinkman, G., Buster, G., Denholm, P., Novacheck, J., Stephan, G., 2018. A National Thermal Generator Performance Database | NREL Data Catalog. https://doi.org/10.7799/1499030.

Rupp, M., Handschuh, N., Rieke, C., Kuperjans, I., 2019. Contribution of country-specific electricity mix and charging time to environmental impact of battery electric vehicles: A case study of electric buses in Germany. Appl. Energy 237, 618–634. https://doi.org/10.1016/j.apenergy.2019.01.059.

Sandmo, T., 2013. The Norwegian Emission Inventory 2013 Documentation of methodologies for estimating emissions of greenhouse gases and long-range transboundary air pollutants.

Sengupta, M., Xie, Y., Lopez, A., Habte, A., Maclaurin, G., Shelby, J., 2018. The National Solar Radiation Data Base (NSRDB). Renew. Sustain. Energy Rev. 89, 51–60. https://doi.org/10.1016/j.rser.2018.03.003.

The World Air Quality Project, 2020. Air pollution in Africa: Real-time air quality index visual map. aqicn.org.

Transport Policy, n.d. US: FUELS: DIESEL AND GASOLINE [WWW Document]. Transport Policy. URL https://www.transportpolicy.net/standard/us-fuels-diesel-and-gasoline/ (accessed 6.20.21).

UETCL, 2020a. Energy Supply and Demand December 2019 – December 2020 – UETCL [WWW Document]. URL https://uetcl.go.ug/energy-supply-and-demand-april-2017-april-2018/ (accessed 6.20.21).

UETCL, 2020b. Load Shedding Trend December 2019 – December 2020 – UETCL [WWW Document]. URL https://uetcl.go.ug/load-shedding-trend-april-2017-april-2018/ (accessed 6.22.21).

UETCL, 2020c. Lira-Gulu-Agago 132 kV T/L (140km) – UETCL [WWW Document]. URL https://uetcl.go.ug/lira-gulu-agago-132-kv-t-l-140km/ (accessed 6.20.21).

UETCL, 2020d. Gulu-Agago-Agago HPP 132kV overhead transmission line & associated substations – UETCL [WWW Document]. URL https://uetcl.go.ug/gulu-agago-agago-hpp-132kv-overhead-transmission-line-associated-substations/ (accessed 6.20.21).

UNBS, 2021. Air quality-Vehicular exhaust emission limits. Kampala.

UNECE, 2018. Road Safety Performance Review Uganda Road Safety Performance Review Uganda UNITED NATIONS ECONOMIC COMMISSION FOR AFRICA UNITED NATIONS ECONOMIC COMMISSION FOR EUROPE Information Service United Nations Economic Commission for Europe.

United Nations, 2020. The Sustainable Development Goals Report 2020. New York City.

United Nations, n.d. Sustainable Development Goal 9 [WWW Document]. UN Sustainable Development Goals. URL https://www.un.org/ga/search/view_doc.asp?symbol=A/RES/70/1&Lang=E (accessed 6.16.21a).

United Nations, n.d. Sustainable Development Goal 13 [WWW Document]. UN Sustainable Development Goals. URL https://sdgs.un.org/goals/goal13 (accessed 6.28.21b).

United Nations, n.d. Sustainable Development Goal 11 [WWW Document]. UN Sustainable Development Goals. URL https://sdgs.un.org/goals/goal11 (accessed 6.16.21c).

U.S. Energy Information Administration, 2016. Uganda - Analysis [WWW Document]. URL https://www.eia.gov/international/analysis/country/UGA (accessed 7.19.21).

Vasic, A.-M., Weilenmann, M., 2006. Comparison of Real-World Emissions from Two-Wheelers and Passenger Cars. Environ. Sci. Technol. 40 https://doi.org/10.1021/es0481023.

Virtanen, P., Gommers, R., Oliphant, T.E., Haberland, M., Reddy, T., Cournapeau, D., Burovski, E., Peterson, P., Weckesser, W., Bright, J., van der Walt, S.J., Brett, M., Wilson, J., Millman, K.J., Mayorov, N., Nelson, A.R.J., Jones, E., Kern, R., Larson, E., Carey, C.J., Polat, İ., Feng, Y., Moore, E.W., VanderPlas, J., Laxalde, D., Perktold, J., Cimrman, R., Henriksen, I., Quintero, E.A., Harris, C.R., Archibald, A.M., Ribeiro, A.H., Pedregosa, F., van Mulbregt, P., Vijaykumar, A., Bardelli, A. Pietro, Rothberg, A., Hilboll, A., Kloeckner, A., Scopatz, A., Lee, A., Rokem, A., Woods, C.N., Fulton, C., Masson, C., Häggström, C., Fitzgerald, C., Nicholson, D.A., Hagen, D.R., Pasechnik, D. v., Olivetti, E., Martin, E., Wieser, E., Silva, F., Lenders, F., Wilhelm, F., Young, G., Price, G.A., Ingold, G.L., Allen, G.E., Lee, G.R., Audren, H., Probst, I., Dietrich, J.P., Silterra, J., Webber, J.T., Slavič, J., Nothman, J., Buchner, J., Kulick, J., Schönberger, J.L., de Miranda Cardoso, J.V., Reimer, J., Harrington, J., Rodríguez, J.L.C., Nunez-Iglesias, J., Kuczynski, J., Tritz, K., Thoma, M., Newville, M., Kümmerer, M., Bolingbroke, M., Tartre, M., Pak, M., Smith, N.J., Nowaczyk, N., Shebanov, N., Pavlyk, O., Brodtkorb, P.A., Lee, P., McGibbon, R.T., Feldbauer, R., Lewis, S., Tygier, S., Sievert, S., Vigna, S., Peterson, S., More, S., Pudlik, T., Oshima, T., Pingel, T.J., Robitaille, T.P., Spura, T., Jones, T.R., Cera, T., Leslie, T., Zito, T., Krauss, T., Upadhyay, U., Halchenko, Y.O., Vázquez-Baeza, Y., 2020. SciPy 1.0: fundamental algorithms for scientific computing in Python. Nature Methods 17. https://doi.org/10.1038/s41592-019-0686-2.

Weldon, P., Morrissey, P., O'Mahony, M., 2016. Environmental impacts of varying electric vehicle user behaviours and comparisons to internal combustion engine vehicle usage - An Irish case study. J. Power Sources 319, 27–38. https://doi.org/10.1016/j.jpowsour.2016.04.051.

Woodyard, D., 2009. Exhaust Emissions and Control, in: Pounder's Marine Diesel Engines and Gas Turbines. Elsevier, pp. 61–86. https://doi.org/10.1016/b978-0-7506-8984-7.00003-5.

World Bank, 2007. Detailed Technology Descriptions and Cost Assumptions.

World Health Organization, 2021. Air pollution data portal [WWW Document]. URL https://www.who.int/data/gho/data/themes/air-pollution (accessed 11.16.21).

World Health Organization, 2018. WHO global ambient air quality database (update 2018). WHO.int.

Yao, Y.C., Tsai, J.H., Ye, H.F., Chiang, H.L., 2009. Comparison of exhaust emissions resulting from cold- and hot-start motorcycle driving modes. J. Air Waste Manag. Assoc. 59 https://doi.org/10.3155/1047-3289.59.11.1339.